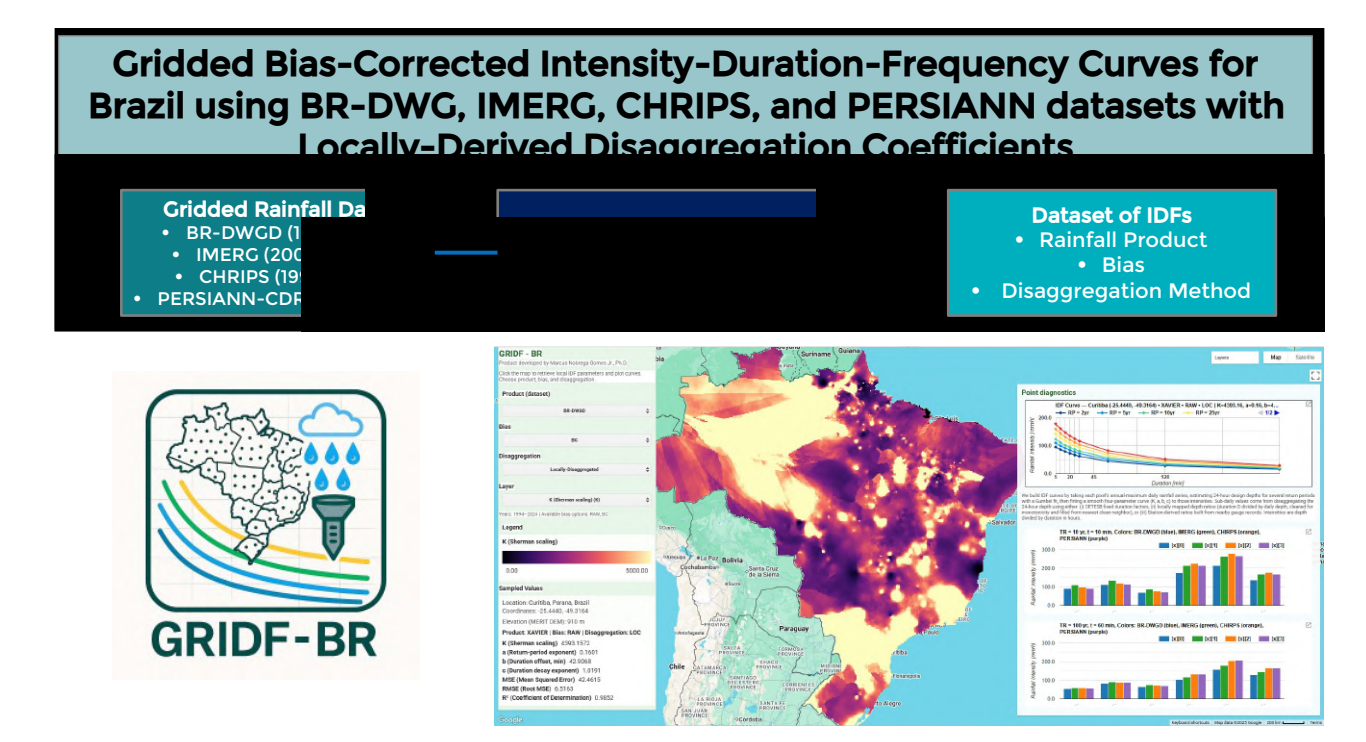
Graphical Abstract

Gridded Bias-Corrected Intensity-Duration-Frequency Curves for Brazil using BR-DWGD, IMERG, CHRIPS, and PERSIANN datasets with Locally-Derived Disaggregation Coefficients

Marcus Nóbrega Gomes Jr.



Highlights

Gridded Bias-Corrected Intensity-Duration-Frequency Curves for Brazil using BR-DWGD, IMERG, CHRIPS, and PERSIANN datasets with Locally-Derived Disaggregation Coefficients

Marcus Nóbrega Gomes Jr.

- A national framework for bias-corrected IDF curves across Brazil is developed.
- Local disaggregation ratios show 1h storms average 56% of daily rainfall totals.
- CETESB constants misestimate extremes by over 30% in convective and orographic regions.
- Multiplicative bias correction at the 98th percentile reduces underestimation of extremes.
- The GRIDF-BR toolbox enables sub-municipality IDF variability estimation.

Gridded Bias-Corrected Intensity-Duration-Frequency Curves for Brazil using BR-DWGD, IMERG, CHRIPS, and PERSIANN datasets with Locally-Derived Disaggregation Coefficients

Marcus Nóbrega Gomes Jr.a,*

^aThe University of Arizona, Department of Hydrology and Atmospheric Sciences, John W. Harshbarger Building, Tucson, 85719, Arizona, United States of America

ARTICLE INFO

Keywords: Rainfall extremes IDF curves Bias correction Disaggregation coefficients Brazil

ABSTRACT

Reliable Intensity-Duration-Frequency (IDF) curves are essential for urban planning, stormwater design, and flood risk management, yet most equations in Brazil remain outdated and rely on spatially uniform disaggregation coefficients. We developed a national framework to generate gridded, biascorrected IDFs by combining daily maxima from BR-DWGD (1994–2024), CHIRPS (1994-2024), PERSIANN-CDR (1994-2024), and IMERG V07 (2000–2024) with sub-daily ratios from 3,165 ANA telemetric stations (see SM for a spatial reference of these). Daily extremes were bias-corrected using exceedances above the 98th percentile, mapped to sub-daily durations, and fitted using the Gumbel distribution in a 4-parameter Sherman equation on a 0.1° grid (0.25° for PERSIANN). Results show that one-hour rainfall represents on average 56% of the daily maximum, while sub-hourly bursts contribute 30-40%. Compared with Environmental Company of the State of São Paul (CETESB) constants, the local typical standard in Brazil, local ratios are lower for very short intervals (5/30 min and 10/30 min lower by 21% and 10%) but higher at longer scales (1 h/24 h is 0.50 versus 0.42, a 16% increase; 6–12 h/24 h are 3–9% higher). Raw gridded rainfall products systematically underestimated extremes, but bias correction improved parity slope agreements in extremes (e.g., BR-DWGD from 0.61 to 1.07; PERSIANN from 0.38 to 0.94). We provide national rasters of Sherman parameters capable of capturing municipal climate variability and the GRIDF-BR Google Earth Engine application for rapid, reproducible IDF retrieval.

1. Introduction

Extreme rainfall events represent one of the most critical hazards for modern societies, with cascading impacts on infrastructure safety, urban mobility, public health, and economic productivity (Handmer et al., 2012; Dodman et al., 2023; Kandalai et al., 2023). Recently, in Rio Grande do Sul, Brazil, floods from April to early May 2024 affected 2.4 million people and left 213 dead or missing, after 444 mm of rain fell in 8 days—652 mm over 35 days and

ORCID(s): 0000-0002-8250-8195X (M.N.G. Jr.)

^{*}Corresponding author

up to 900 mm in some areas (Collischonn et al., 2025; Simoes-Sousa et al., 2025). The design of drainage systems, flood defenses, and other water-related infrastructure relies fundamentally on Intensity–Duration–Frequency (IDF) curves, which summarize the statistical relationship between storm intensity, duration, and recurrence (Butcher et al., 2021). Outdated or poorly calibrated IDFs can lead to underestimation of design storms, resulting in insufficient capacity of storm sewers, frequent road flooding, or even structural failures in dams and levees (Bibi and Tekesa, 2023; Cook et al., 2020). The economic costs of such misestimations are amplified in densely populated urban centers, where infrastructure resilience directly affects millions of people. Climate change is expected to exacerbate these risks by altering both the frequency and intensity of extreme daily and sub-daily precipitation (Mascaro et al., 2025; Arnbjerg-Nielsen et al., 2013; Tamm et al., 2023; Ballarin et al., 2024), yet in practice, many regions still lack updated IDFs even for the current climate, leaving urban planning and risk management reliant on obsolete design standards.

A major constraint on developing reliable IDFs is the availability of high-quality, long-term subdaily rainfall data (Yan et al., 2021). Short-duration records are indispensable for designing systems sensitive to high-intensity bursts, such as urban stormwater networks, but in many countries, such data remain limited in spatial coverage and temporal continuity. Breaks in measurement, inconsistent maintenance of pluviographs, and relatively recent deployment of automatic stations contribute to fragmented datasets that are often too short for robust extreme value analysis (das Neves Almeida et al., 2025). Even at the daily scale, rain gauge density can be insufficient to resolve spatial variability across diverse climatic regions, resulting in large ungauged areas where IDFs must be extrapolated. This lack of observational rainfall depths poses significant challenges for urban planning, hydrological modeling, and the development of reliable regional design standards.

In this context, remote sensing technologies have emerged as an important complement to ground-based observations. Weather radar networks provide high-resolution coverage at regional scales (Ghebreyesus and Sharif, 2021), while satellite-based precipitation estimates such as those from passive microwave and infrared sensors extend observations to national and continental domains (Ombadi et al., 2018; Venkatesh et al., 2022; Mianabadi, 2023; Lau and Behrangi, 2022; Alsumaiti et al., 2023). These products make it possible to infer IDF relationships in regions where ground data are sparse or unavailable, offering new opportunities for resilient infrastructure design in data-scarce environments. However, radar and satellite products are not free from limitations: they often carry systematic biases, underestimate extremes in convective systems, or misrepresent orographic enhancement. For this reason, bias correction against ground data is essential before such products can be applied to engineering design.

In Brazil, where densely populated urban areas coexist with flood-prone river basins, reliable and spatially consistent Intensity–Duration–Frequency (IDF) curves are critical for the design of resilient hydraulic infrastructure (Stein et al., 2024). Outdated or poorly calibrated IDFs can substantially underestimate extreme rainfall magnitudes, leading to insufficient drainage capacity, structural failures, and heightened economic and social risks during flood events. Historically, IDF derivation across the country has relied on heterogeneous methodologies, with differences in record length, probabilistic distribution choice, and quality control procedures. A particularly limiting step has been the conversion from daily to sub-daily durations, which is often performed using constant disaggregation coefficients recommended by the CCETESB (*Environmental Company of the State of São Paulo*) (de Saneamento et al., 1986). These coefficients, derived from a limited number of pluviographic stations in southeastern Brazil, have been applied nationwide without

regional validation. As a result, they might fail to capture the marked spatial variability associated with storm type, convective activity, and orographic effects, leading to systematic biases in short-duration rainfall estimates. Although a few studies have attempted to refine these ratios using local pluviographic or automatic station data (Carvalho Abreu et al., 2023; Caldeira et al., 2015), CETESB's constants remain the default in many design guidelines due to the absence of a spatially explicit, nationally consistent alternative.

1.1. Literature Review

In Brazil, numerous efforts have been undertaken to estimate Intensity-Duration-Frequency (IDF) relationships, generally constrained to specific states or municipalities and based on locally available pluviometric or pluviographic records. Several studies have relied on daily Annual Maximum Series (AMS) of daily rainfall depth combined with standard disaggregation coefficients from CETESB to obtain sub-daily intensities (Campos et al., 2017; de Souza et al., 2016; Ballarin et al., 2022b; Lima et al., 2021; Back et al., 2020), while others have derived local coefficients from high-resolution pluviograph data to improve accuracy (Almeida et al., 2025; Carvalho Abreu et al., 2023; de Bodas Terassi et al., 2023; Penner et al., 2023). These coefficients, determined by CETESB, are widely used in the derivations of IDF curves for Brazil. In states such as Rio Grande do Sul, Sao Paulo, Paraná, Rondônia, and Paraíba, IDF curves have been estimated using probability distributions including Gumbel, GEV, Kappa, and Log-Pearson III, often with spatial interpolation techniques such as inverse distance weighting, Voronoi polygons, or Ordinary Cokriging (Rodrigues et al., 2024, 2023; Aragão et al., 2024; Pansera and Gomes, 2025; de Souza et al., 2016; Coelho et al., 2023). These works have generated valuable spatial datasets of IDF parameters, yet the statistical methods, record length requirements, and spatial resolution vary considerably among regions.

The approaches adopted also differ in their treatment of temporal variability. Most studies assume stationarity in extreme rainfall statistics (Rodrigues et al., 2024, 2023; Aragão et al., 2024; Pansera and Gomes, 2025; de Souza et al., 2016; Lima et al., 2021; Coelho et al., 2023; Back et al., 2020; Boulomytis et al., 2018; Penner et al., 2023), but recent works have explored nonstationary modeling in response to observed or projected climate change (de Souza Costa et al., 2020; Silva et al., 2023; Nunes et al., 2021).

At the national scale, an unprecedented effort has been made to compile and harmonize IDF parameters from 370 publications into an open database covering 6,550 locations (Torres et al., 2025). This dataset consolidates disparate sources and provides a foundation for broader analyses, but it inherits the methodological inconsistencies of its constituent studies, including heterogeneous statistical models, disaggregation approaches, and validation procedures. Furthermore, several state-level investigations have been limited by sparse gauge networks, short historical records, or the absence of pluviographic data, leading to uncertainties in short-duration estimates (Carvalho Abreu et al., 2023; Lima et al., 2021; Boulomytis et al., 2018; Penner et al., 2023). These limitations are particularly acute in the North and Northeast, where long-term high-resolution rainfall measurements are scarce (de Bodas Terassi et al., 2023; de Souza Costa et al., 2020).

1.2. Paper Objectives and Contributions

This methodological fragmentation, as aforementioned, presents a critical gap: While regional and local IDF curves exist for many parts of Brazil, there is no unified, methodologically consistent framework to estimate IDF relationships or to derive disaggregation coefficients for the entire

country, aiming to provide better estimates of sub-daily rainfall extremes in poorly gauged areas. The heterogeneity in input data resolution, statistical modeling choices, spatial interpolation methods, and temporal assumptions hampers comparability and integration. In this context, the development of a national-scale IDF estimation approach based on gridded rainfall datasets offers a pathway to ensure spatial continuity and methodological uniformity, especially in data-scarce areas. Such a framework would support resilient infrastructure design and water resources planning and management.

The primary objective of this study is to develop a consistent, nationwide framework for updating rainfall Intensity—Duration—Frequency (IDF) curves for Brazil. To this end, we integrate BR-DWGD daily maxima (1994–2024) (Xavier et al., 2022) with locally derived sub-daily disaggregation coefficients from ANA's automatic network, while also incorporating satellite-based products (IMERG (Huffman et al., 2023), PERSIANN-CDR (Ashouri et al., 2015), and CHIRPS (Funk et al., 2015)) to improve coverage in regions with sparse gauge density and to provide local comparative analysis of different products, enhancing uncertainty analysis. Beyond producing harmonized gridded IDFs, we further implement an open-access toolbox on the Google Earth Engine platform, namely *Gridded Intensity Duration Frequency - Brazil* (GRIDF - BR) available at https://gridf-470516.projects.earthengine.app/view/gridf-br, enabling rapid evaluation of IDFs under different scenarios, including raw versus bias-corrected data, alternative disaggregation strategies, and cross-product comparisons.

2. Methodology

2.1. Study Area

Brazil spans over 8.5 million km² across a wide latitudinal range (5°N-34°S) and longitudinal extent (34°W-74°W), resulting in pronounced geographical, climatic, and hydrological diversity as presented in Fig. 1. The country encompasses multiple Köppen climate zones, from humid equatorial (Af, Am) conditions in the Amazon Basin, with annual rainfall often exceeding 2,500 mm, to semi-arid (BSh) regions in the Northeast where totals frequently fall below 800 mm. Tropical savanna (Aw) climates dominate much of central Brazil, while humid subtropical (Cfa, Cfb) conditions prevail in the South. Rainfall regimes are driven by a combination of largescale and regional atmospheric systems, including the Intertropical Convergence Zone (ITCZ), South Atlantic Convergence Zone (SACZ), mesoscale convective systems, and mid-latitude frontal systems, with significant modulation by orographic features such as the Serra do Mar and Serra da Mantiqueira. These processes produce strong spatial and temporal variability in precipitation extremes, with urban flash flooding recurrent in densely populated areas such as São Paulo, Rio de Janeiro, and Belo Horizonte, and widespread riverine flooding in major basins like the Amazon, Paraná, and São Francisco. This heterogeneity in climate drivers and hazard exposure highlights the need for spatially explicit and locally calibrated Intensity-Duration-Frequency (IDF) curves to support climate-resilient hydraulic infrastructure design across the country.

2.2. Rainfall Datasets

2.2.1. BR-DWGD

We employed the Brazilian Daily Weather Gridded Dataset (BR-DWGD) (Xavier et al., 2022), which provides daily precipitation fields at 0.1° (≈ 11 km at the equator) resolution. Originally spanning 1961–2020, the dataset was extended by (Xavier et al., 2022) to January 2024 and is based

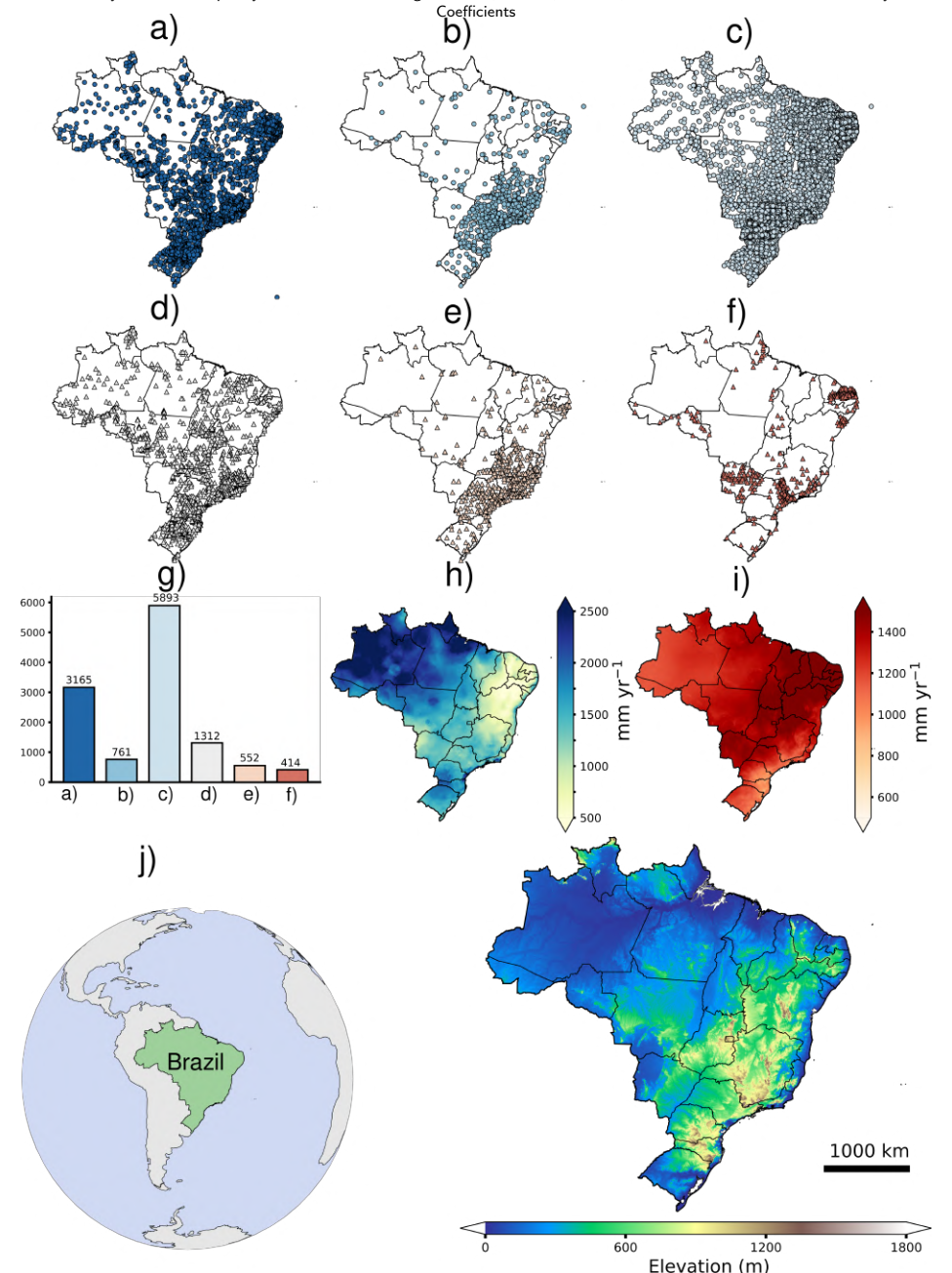


Figure 1: Study area and spatial distribution of rain-gauge stations for hydro-climatic analysis in the context of Brazil. (a–c) Locations of station sets (data without treatment) for the ANA sub-daily stations (a), and stations used in Torres et al. (2025) to derive IDFs with sub-daily data (b) and with disaggregation methods (c). Similarly, parts (d-f) are the treated rain gauge stations for the same cases of (a-c) ,following quality control checks. Plot (g) shows the number of stations of each case, and (h-j) shows national annual mean precipitation (1994–2024 using BR-DWGD at 0.1° resolution), evapotranspiration (from remotely sensed products at 0.1° resolution), and 90-m DEM using MERIT DEM.

on a dense network of rain gauges from multiple national and regional agencies. Station quality control, including consistency checks, outlier detection, and cross-validation with neighboring gauges, after which spatial interpolation was performed using Angular Distance Weighting (ADW) to better capture complex rainfall gradients (Xavier et al., 2022).

2.2.2. IMERG (Integrated Multi-satellitE Retrievals for GPM)

The Integrated Multi-satellitE Retrievals for GPM (IMERG, Version 07) (Huffman et al., 2023) provides global precipitation estimates by merging passive-microwave observations from the GPM constellation with geostationary infrared data and monthly gauge analyses. It offers near-global coverage (90° N–90° S) at 0.1° spatial and 30-minute temporal resolution from June 2000 to the present, with three processing streams: *Early* and *Late* runs for near-real-time monitoring, and the gauge-adjusted *Final* run recommended for hydrological applications. IMERG data are distributed via NASA GES DISC, PPS, and Google Earth Engine, with precipitation reported as rain rate (mm h⁻¹). Despite improvements in Version 07, limitations remain, including underestimation of orographic enhancement, smoothed convective peaks, and detection errors in light or warm-rain events. Furthermore, only the final run applies gauge correction, making local validation and bias adjustment essential when using IMERG for engineering design and IDF curve estimation.

2.2.3. CHIRPS (Climate Hazards Group InfraRed Precipitation with Station Data)

The Climate Hazards Group InfraRed Precipitation with Station Data (CHIRPS) (Funk et al., 2015) provides quasi-global rainfall estimates from 1981 to the present, spanning 50° S−50° N at 0.05° (≈5 km) spatial resolution. It is generated by blending infrared-based cold-cloud duration fields with in situ rain gauge observations from multiple networks, thereby reducing systematic biases common to purely satellite products while retaining fine spatial detail. CHIRPS is openly available in GeoTIFF and NetCDF formats through the Climate Hazards Center and on Google Earth Engine (UCSB-CHG/CHIRPS/DAILY), with daily, pentadal, and monthly aggregations. Known limitations include underestimation of warm-rain processes and orographic enhancement, as well as regionally variable gauge density for bias correction, leading to larger errors in convective, mountainous, and coastal regions. Nonetheless, its long record, relatively high resolution, and integration of ground data have established CHIRPS as a widely used dataset for drought monitoring, climate variability analysis, and hydrological modeling across the tropics and subtropics.

2.2.4. PERSIANN-CDR (Precipitation Estimation from Remotely Sensed Information using Artificial Neural Networks – Climate Data Record)

The Precipitation Estimation from Remotely Sensed Information using Artificial Neural Networks–Climate Data Record (PERSIANN-CDR) (Ashouri et al., 2015) provides global daily precipitation estimates from 1983 to the present at 0.25° spatial resolution. Produced by the Center for Hydrometeorology and Remote Sensing (CHRS), it applies an artificial neural network to geostationary infrared imagery, followed by monthly bias adjustment using the Global Precipitation Climatology Project (GPCP) product to ensure temporal consistency. PERSIANN-CDR is distributed in NetCDF format through NOAA's NCEI and the CHRS Data Portal, and its long record makes it well suited for climate variability analyses, drought monitoring, and hydrological trend studies. Limitations include difficulties in representing warm-rain processes, uncertainties in convective regimes, and underestimation of orographic enhancement, while the coarser 0.25° resolution smooths localized extremes compared to finer-scale datasets such as IMERG or CHIRPS.

Nevertheless, its temporal length, homogeneity, and gauge-adjusted bias correction provide a robust foundation for climatological and hydrological applications, especially when used in combination with higher-resolution or ground-based datasets.

2.2.5. Annual Maxima Extraction

To construct annual maximum series for Intensity–Duration–Frequency (IDF) analysis, we first downloaded daily precipitation data in NetCDF format from each gridded product considered in this study. The analysis period was set to 1994–2024 for BR-DWGD, CHIRPS, and PERSIANN-CDR, while for IMERG the record was limited to 2000–2024 due to its later availability. For each grid cell, the AMS was extracted by scanning the full daily series within each calendar year. This procedure was applied independently to all datasets at their native spatial resolution before subsequent spatial harmonization to the 0.1° target grid, except for PERSIANN-CDR, which was made for a 0.25° grid.

2.2.6. High-Resolution Sub-Daily Rainfall Data

High-resolution rainfall observations were obtained from the Brazilian National Water Agency (ANA) telemetric network through its automatic data retrieval platform. The dataset includes records from 3,165 stations distributed across Brazil, with temporal resolutions ranging from 15 minutes to 1 hour, depending on station configuration and availability. Data was retrieved from 01/01/2010 to 01/01/2024. Given the relatively limited distribution of stations, we opted to remove stations with more than 30% missing data or less than 4 years of data, which were not considered. In addition, to remove clear measurement errors in the analysis, stations with recorded values larger than 300 mm / 15-min time-steps had their values dismissed. In this study, we focus on recent rainfall sub-daily characteristics rather than collecting old inactive stations, as presented in previous articles that developed disaggregation coefficients (Torres et al., 2025).

Custom MATLAB scripts were developed to automate the retrieval from ANA API, perform quality control, and organize these high-frequency records in a dataframe. For each station, subdaily rainfall series were processed to extract annual maximum precipitation for durations matching those defined in the CETESB methodology (15, 30, 60 minutes, 6, 8, 10, 12, and 24 hours). Local disaggregation coefficients were then computed as the ratio between the corresponding maximum precipitation observed at each sub-daily duration and the annual maximum daily rainfall.

2.3. Disaggregation Coefficients

2.3.1. Derivation of local disaggregation coefficients

Local disaggregation coefficients were derived from quality-controlled sub-daily rainfall records obtained from the National Agency of Water (ANA) telemetric network. For each station, daily totals were first accumulated using a fixed 24-hour window anchored at 07:00 local time, the typical time at which measurements of pluviometer stations are taken. The maximum daily rainfall observed over the record was then identified as the reference value against which sub-daily maxima were scaled.

To compute daily volumes, a time-window shift starting daily at 7 a.m. was used as a proxy for daily rainfall to determine disaggregation coefficients from daily to 24-h. Sub-daily maxima were extracted by applying a continuous moving window to the high-resolution rainfall series. For each target duration in the set of 15, 30, 60, 360, 480, 600, 720, and 1,440 minutes, the largest rainfall accumulation across the entire observation period was recorded. The disaggregation

coefficient for a given duration was then defined as the ratio between this sub-daily maximum and the corresponding daily maximum. These dimensionless ratios provide a direct measure of how extreme sub-daily rainfall relates to daily extremes at each station and form the basis for subsequent IDF curve derivation.

To ensure consistency and quality, stations were retained only if they satisfied the following criteria: (i) at least four distinct hydrologic years of valid sub-daily data, (ii) no daily total exceeding 500 mm, (iii) at most one calendar year with all daily totals equal to zero (as a proxy for sensor or ingest failure), and (iv) strictly increasing disaggregation ratios across durations,

$$r_{15} < r_{30} < r_{60} < r_{360} < r_{480} < r_{600} < r_{720} < r_{1440},$$
 (1)

within a numerical tolerance $\varepsilon = 10^{-6}$. Although nondecreasing (\leq) behavior is physically admissible, plateaus often arise when the strongest event has a duration shorter than the longer windows, producing degenerate r_t values that flatten for larger t. Enforcing a strict increase yielded better-conditioned duration scaling and more stable IDF fits.

Because the minimum observational resolution of the stations was 15 minutes, direct estimates for shorter durations (5, 10, 20, and 25 minutes) were not possible, unless a data-driven model is used. To extend the coefficient set, a logarithmic model of the form $c = a \ln(t) + b$ was fitted to the observed coefficients for durations equal to or longer than 15 minutes, up to 24 hours (Silveira, 2000). The fitted curve was then used to predict coefficients at t = 5, 10, 20, and 25 minutes. To guarantee physical consistency, monotonicity constraints were enforced such that $0 \le c_5 \le c_{10} \le c_{15}$ and $c_{15} \le c_{20} \le c_{25} \le \min(c_{30}, 1)$. When the raw logarithmic fit violated these constraints or produced non-finite or negative estimates, only the offending predictions were replaced using empirically derived ratio fallbacks from the subset of stations with valid fits (see Sup. Material for reference to the determination of these fallbacks). Specifically, the fallback ratios applied were $c_{10} = 0.817 \, c_{15}, \, c_5 = 0.510 \, c_{10}$ (or, if c_{10} was unavailable, $c_5 = 0.417 \, c_{15}$), $c_{20} = 0.830 \, c_{30}$, and $c_{25} = 0.918 \, c_{30}$. After applying these corrections, any residual violations were clipped to the nearest admissible bound to enforce $0 \le c_5 \le c_{10} \le c_{15} \le c_{20} \le c_{25} \le \min(c_{30}, 1)$. Stations requiring fallback or clamping were labeled *violated-fit*, whereas those satisfying all constraints without intervention were labeled *ok-fit*.

Out of the 594 stations with a minimum resolution of 15 minutes, 189 yielded consistent logarithmic fits, while 397 exhibited at least one violation for shorter durations. All results were systematically flagged according to their performance, and we recommend cautious use of stations labeled as *violated-fit* to avoid unrealistic IDF parameterizations. The final dataset was delivered both as a georeferenced shapefile and as a tabular .csv file, available at https://github.com/marcusnobrega-eng/GRIDF

2.3.2. Interpolation and Treatment of Numerical Artifacts

To provide continuous spatial coverage of disaggregation coefficients across Brazil, we applied Inverse Distance Weighting (IDW) interpolation to the at-station sub-daily rainfall ratios derived from ANA's high-resolution rainfall network. Interpolation was performed on a 0.1° grid with a power parameter of two and a neighborhood of the five nearest stations. This method was selected for its simplicity, reproducibility, and widespread use in hydrological applications where unevenly distributed gauge networks are available.

A known limitation of interpolated disaggregation surfaces is the potential introduction of numerical artifacts, particularly the violation of the monotonicity condition that requires sub-daily disaggregation ratios to increase with duration. Such non-physical behavior may arise in sparsely gauged areas or in transitional climatic zones where interpolation blends contrasting regimes. To address this issue, we adopted a hybrid strategy: when interpolated ratios at a given grid cell did not satisfy the monotonicity criterion, the Intensity–Duration–Frequency (IDF) fitting was instead performed using the disaggregation coefficients of the nearest observation grid cell that met all screening requirements. While this approach ensures physically consistent IDF curves for practical applications, we also make the interpolated rasters available in the database as supplementary products. These rasters are valuable for visualizing large-scale spatial patterns and conducting exploratory analyses, but users are cautioned that grid cells affected by non-monotonic artifacts should not be directly applied in design studies without further inspection.

2.3.3. CETESB Disaggregation Coefficients

As a reference scenario, we adopt the fixed-duration rainfall ratios provided by the Environmental Company of the State of São Paulo (CETESB) (de Saneamento et al., 1986), which have been traditionally used in Brazilian hydraulic design standards using IDF curves. These coefficients express the proportion of maximum precipitation at sub-daily durations relative to the maximum daily rainfall and are assumed spatially invariant across the country. The fixed ratios are: 0.248 for 15 min, 0.354 for 30 min, 0.479 for 1 h, 0.821 for 6 h, 0.889 for 8 h, 0.939 for 10 h 0.956 for 12 h, and 1.14 for 24 h. Although widely applied in engineering practice, these constants were originally derived from a limited regional dataset and may not accurately represent local rainfall dynamics in diverse climatic regions of Brazil, thereby motivating the present comparison with locally derived disaggregation coefficients. For the IDFs fitted with CETESB coefficients, all disaggregation durations were used.

2.4. Multiplicative Bias Correction and Percentile Analysis

To evaluate and correct systematic deviations in satellite- and reanalysis-based rainfall products, multiplicative bias factors were derived using matched pairs of annual maximum daily precipitation from ANA pluviometric stations and collocated grid cells. For each year in the study period, the largest daily rainfall was extracted at every station using the HydroBr tool (Carvalho, 2020) and compared with the corresponding product value at the same location. The ratio of observed to gridded maxima defines a multiplicative factor that rescales product estimates toward the station-based reference. This approach preserves the temporal structure of the gridded series while correcting systematic magnitude errors (Alsumaiti et al., 2023).

Because Intensity–Duration–Frequency (IDF) analyses are primarily driven by the upper tail of the rainfall distribution, bias correction was further assessed across percentile thresholds rather than only at the mean or median. In particular, emphasis was placed on the 98th percentile, which represents the long tail of the distribution where the most hydrologically relevant extremes occur. This choice ensures that the correction improves the representation of rare but impactful events, which directly govern return period estimates and hydraulic design criteria. Diagnostic plots and validation metrics were therefore computed across percentiles, with particular attention to the upper decile, to confirm that the corrected products reproduce extreme rainfall behavior rather than simply adjusting central tendencies. By explicitly targeting the long tail of the distribution,

the methodology strengthens the reliability of corrected rainfall fields for IDF curve estimation and flood risk assessment.

2.4.1. Computation of Bias Factors

Bias factors were computed to quantify the systematic difference between gridded rainfall products and station observations, focusing on the upper tail of the distribution relevant for IDF estimation. For each station *i*, daily precipitation values were paired with the corresponding grid cell from each product. Only values exceeding the 98th percentile of the station's distribution were retained, ensuring that the correction targets extremes rather than central tendencies.

For each exceedance pair j at station i, the instantaneous ratio was calculated as

$$\zeta_{ij} = \frac{P_{ij}^{\text{station}}}{P_{ij}^{\text{product}}}.$$
 (2)

The representative bias factor for station i was then defined as the mean across all N_i exceedances:

$$\zeta_i = \frac{1}{N_i} \sum_{i=1}^{N_i} \zeta_{ij}. \tag{3}$$

Values of $\zeta_i > 1$ indicate systematic underestimation of extremes by the product, while $\zeta_i < 1$ indicate overestimation. To ensure stability and robustness, additional filters were applied: annual maxima below 1 mm day⁻¹ were excluded, ratios outside the range [0.1, 10] were clipped, and stations with fewer than ten valid exceedances were removed from the analysis.

2.4.2. Spatial Interpolation of Bias Factors

Station-level bias factors were interpolated to continuous grids using inverse-distance weighting (IDW). The interpolated field can be estimated as:

$$\zeta(x,y) = \frac{\sum_{i=1}^{k} w_i(x,y) \, \zeta_i}{\sum_{i=1}^{k} w_i(x,y)}, \qquad w_i(x,y) = \frac{1}{d_i(x,y)^p},\tag{4}$$

where $d_i(x, y)$ is the distance from station *i* to the grid point. The parameters used were p = 2 for the distance decay and k = 5 for the number of neighbors. Interpolation was carried out separately for each dataset, with PERSIANN bias factors assigned to a 0.25° grid and the others to a 0.1° grid.

2.4.3. Bias Correction of Annual Maxima Fields

For each rainfall product, a gridded field of bias factors was obtained from the IDW interpolation. This field was then used to correct the raw annual maxima as

$$P^{\text{corrected}}(x, y) = \zeta(x, y) \cdot P^{\text{product}}(x, y). \tag{5}$$

This multiplicative adjustment rescales the rainfall extremes in each dataset to better match gauge-based reference values.

2.4.4. Validation and Diagnostics

Bias-corrected datasets were evaluated using graphical and statistical diagnostics. Scatter plots of observed versus gridded annual maxima were constructed before and after correction, with the 1:1 line as reference. Density plots illustrate the concentration of points across the value range. The coefficient of determination (R^2), mean bias, root-mean-square error (RMSE), and the Kolmogorov–Smirnov statistic (D and associated p-value) were computed to test distributional similarity. These diagnostics provide complementary views of the effectiveness of the bias correction, focusing both on pointwise agreement and on the distribution of extremes.

2.5. Extreme value analysis (Gumbel)

Annual daily maxima at each pixel are modeled with the Gumbel (Type I) distribution (Cooray, 2010), a standard choice for block maxima that avoids the instability of estimating a shape parameter from short records. With X the annual maximum depth, the cumulative distribution function is

$$F_G(x; \mu, \beta) = \exp\left[-\exp\left(-\frac{x-\mu}{\beta}\right)\right],\tag{6}$$

where μ and $\beta > 0$ are location and scale. Parameters are estimated by method of moments for numerical robustness and reproducibility in large spatial fits. Let m and s denote the sample mean and unbiased standard deviation of the annual maxima:

$$\widehat{\beta} = \frac{s}{\pi/\sqrt{6}}, \qquad \widehat{\mu} = m - \gamma \,\widehat{\beta}, \tag{7}$$

with Euler's constant $\gamma \approx 0.57721$. Return levels use the reduced variate

$$y_T = -\ln\left[-\ln\left(1 - \frac{1}{T}\right)\right],\tag{8}$$

giving the T-year quantile

$$x_T = \hat{\mu} + \hat{\beta} y_T, \tag{9}$$

evaluated for $T \in \{2, 5, 10, 25, 50, 75, 100\}$ years to remain within a defensible extrapolation range relative to record length and to represent the typical return periods used in urban drainage design.

Goodness-of-fit is screened by a Kolmogorov–Smirnov (KS) test applied to the fitted CDF (Berger and Zhou, 2014). With F_n the empirical CDF (plotting positions $(i - \frac{1}{2})/n$ on the ordered sample), the statistic and p-value are

$$D_n = \sup_{x} |F_n(x) - F_G(x; \hat{\mu}, \hat{\beta})|, \tag{10}$$

$$\lambda = (\sqrt{n} + 0.12 + 0.11/\sqrt{n})D_n, \qquad p \approx 2\sum_{j=1}^{\infty} (-1)^{j-1} e^{-2j^2 \lambda^2}, \tag{11}$$

and the model is rejected at level $\alpha = 0.05$ when $p < \alpha$. Resulting daily return levels are subsequently mapped to subdaily intensities using externally specified disaggregation factors.

2.6. IDF Curve Fitting

We fitted pixelwise Intensity–Duration–Frequency (IDF) relations using the four-parameter Sherman model (Sherman, 1931),

$$i(t, RP) = \frac{K RP^a}{(b+t)^c},\tag{12}$$

where i is intensity (mm h⁻¹), t is duration (min), RP is the return period (yr), and (K, a, b, c) are empirical parameters. For each dataset (BR-DWGD, IMERG, CHIRPS, and PERSIANN-CDR) we constructed annual-maximum daily (24 h) series at the native grid, both in raw and bias-corrected form. Daily extremes were modeled with the Gumbel distribution previously described.

Sub-daily design depths were generated by scaling $P_{24}(RP)$ with duration-specific disaggregation ratios and converting to intensities. We evaluated three disaggregation modes: (i) CETESB, using fixed national ratios; (ii) RASTER, using spatially continuous ratio fields obtained by IDW interpolation of station-based ratios with monotonicity enforcement and nearest-neighbor repair of problematic pixels; and (iii) STATION, assigning to each grid cell the ratio vector from the nearest "ok-fit" telemetric gauge. Durations were $t \in \{5, 10, 15, 20, 25, 30, 60, 360, 480, 600, 720, 1440\}$ min; and sub-hourly ratios follow the station-calibrated/log-extended scheme described earlier for durations outside multiples of the station duration. This workflow was run for every dataset and for both raw and bias-corrected annual maxima, yielding paired families of sub-daily design intensities across return periods and durations.

Sherman parameters (K, a, b, c) were estimated per pixel by nonlinear least squares in log space, using a linear (Bernard-type) regression as a warm start and bounded optimization to ensure physical plausibility. Specifically, we minimized the sum of squared residuals between \log_{10} of the gridded design intensities and the model $\log_{10}(KRP^a) - c \log_{10}(b+t)$, with lower/upper bounds K > 0, $0 \le a \le 1$, b > 0, and $0 < c \le 5$. When available, 1sqcurvefit (trust-region-reflective) was used; otherwise, a derivative-free fallback (fminsearch) on a reparameterized space ensured robustness. For each fit we stored (K, a, b, c) and diagnostics (MSE, RMSE, and R^2), producing georeferenced rasters for all datasets, disaggregation modes, and bias-correction states suitable for city- or catchment-level IDF extraction.

2.7. Context of Existing IDF Dataset

The comprehensive national IDF database compiled by Torres et al. (2025) provides an unprecedented collection of 6,550 station-based equations across Brazil, serving as an important benchmark for hydrologic and hydraulic studies. However, the temporal coverage of the underlying records for IDFs delimited with pluviography data is limited. On average, for IDFs fitted with pluviographs, the rainfall series used for the fittings span only 16.7 ± 7 years, with most equations beginning in 1980 and extending, on average, until 1997 for the IDFs based on pluviographic stations. This indicates that a substantial portion of the database reflects climatic conditions of the late 20th century rather than more recent decades, during which both observational networks and climate variability have evolved significantly.

The relatively short record lengths and the absence of updates beyond the 1990s suggest that many of the equations in Torres et al. (2025) dataset may underestimate or misrepresent current rainfall extremes (Ballarin et al., 2022a). Consequently, while invaluable as a useful reference, this dataset highlights the need for a unified methodology based on long-term, quality-controlled, and up-to-date observations. In this context, our study provides a complementary perspective by generating IDFs from satellite products and rain gauge-based observations.

From a national archive of 6,586 IDFs parametrizations available in Torres et al. (2025), we built two analysis subsets. First, the "standard" network comprised 762 stations with ≥ 10 years of observations valid for all durations; after applying completeness and quality filters, this was reduced to 552 stations. The standard stations were derived with sub-daily rainfall data, and therefore, no disaggregation coefficients were used. The data used to derive these disaggregation coefficients is not readily available; therefore, no quality control was performed on the derived IDF curves from this method. Instead, we assumed the published values from Torres et al. (2025). Because multiple gauges occasionally fell within the same 0.1° grid cell, we selected a single representative gauge per pixel (after resampling to the analysis grid), yielding 390 stations used for the spatial interpolation. Second, for the daily/disaggregation IDFs that used various methods for disaggregation coefficients, we adopted a stricter screening—requiring ≥ 30 years of record and removing dubious values according to our QC threshold, which reduced the original 5,894 stations to 414 stations QC checked stations. The resulting stations were later used to compare newly developed IDFs generated with GRIDF and compare them to the existing database.

3. Results

3.1. Disagregation Coefficients

The spatial distribution of disaggregation coefficients derived from ANA's sub-daily gauge network for durations ranging from 15 minutes to 24 hours, expressed as ratios relative to the daily maximum, is presented in Figure 2. The network spans all major regions of Brazil, with higher station density in the South, Southeast, and Northeast, and sparser coverage in the Amazon and interior North. Results indicate that short durations already account for a representative fraction of daily extremes: for example, the 1-hour duration captures on average 56% of the daily maximum, underscoring the dominance of intense convective bursts in shaping daily totals. The 15- and 30-minute durations also contribute significantly, with mean ratios of 0.30 and 0.41, respectively, while longer durations progressively approach unity, with 0.87 at 6 hours, 0.98 at 12 hours, and 1.14 at 24 hours. This pattern highlights that sub-hourly to hourly extremes are not negligible, but instead represent a substantial share of daily rainfall, particularly in regions affected by short-lived convective storms. The variability observed at intermediate durations reflects the influence of contrasting storm regimes across Brazil, while the number of extracted maxima per station reveals heterogeneous data availability, with some gauges contributing over 200 events and others far fewer.

Figure 3 illustrate the spatial distribution of sub-daily rainfall ratios across Brazil, obtained by interpolating at-station coefficients from the ANA telemetric network to a 0.1° grid using inverse-distance weighting. The maps show how rainfall accumulated over short reference durations (from 5 minutes up to 12 hours) compares with longer benchmarks, highlighting the temporal scaling of extremes across diverse climatic regions. For the shortest intervals (5–15 minutes relative to 30 minutes), higher ratios are evident in the North and Northeast, reflecting the dominance of intense

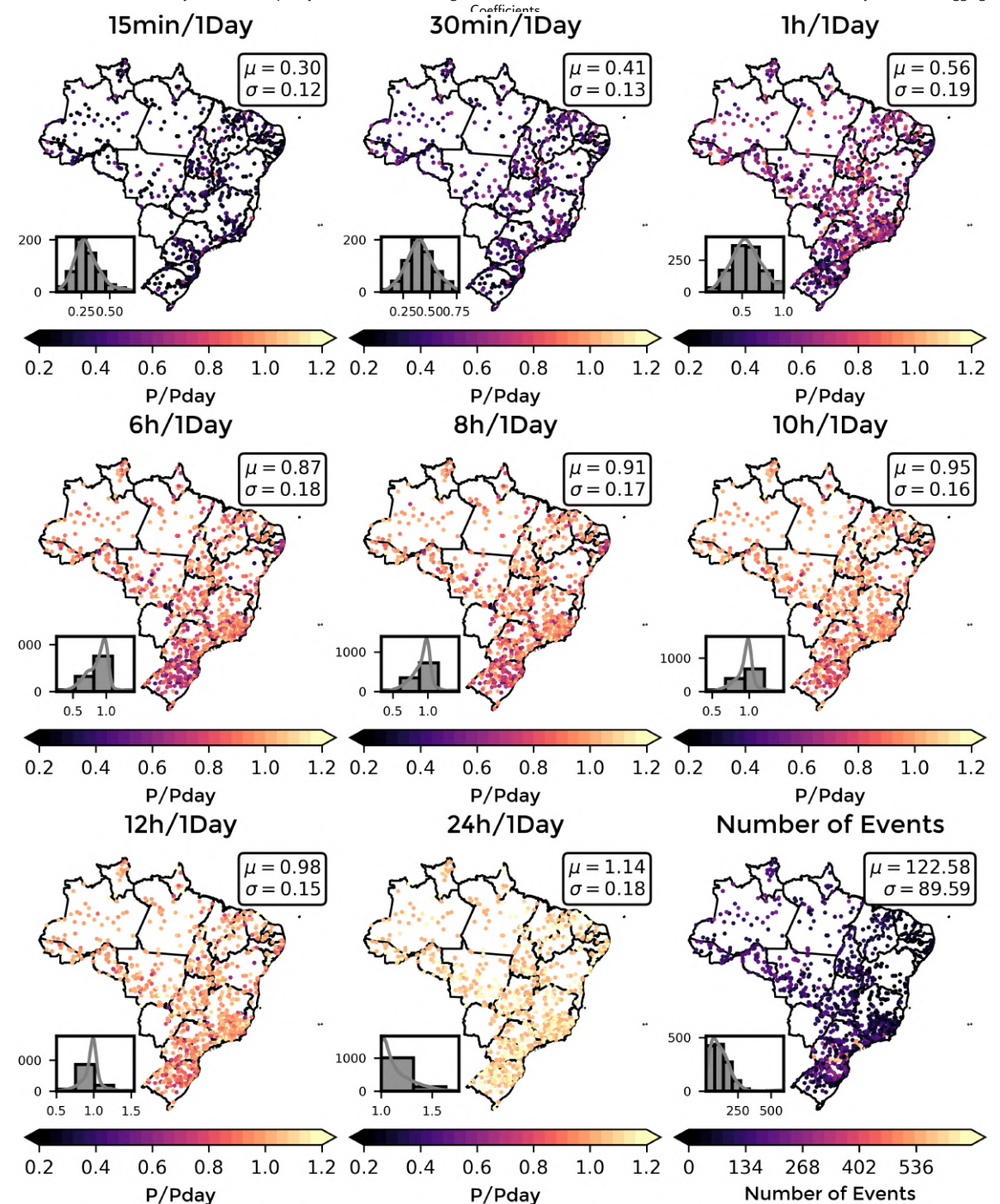


Figure 2: At-station disaggregation coefficients for Brazil using ANA stations.

convective bursts that contribute disproportionately to short-duration rainfall. Conversely, lower values are found in the South, where frontal systems and stratiform precipitation spread totals more evenly over time. The transition from 30 minutes to 1 hour, and from 1 hour to 24 hours, shows that

Time Relation	5min/ 30min	10min/ 30min	15min/ 30min	20min/ 30min	25min/ 30min	30min/ 1h	1h/ 24h	6h/ 24h	8h/ 24h	10h/ 24h	12h/ 24h	24h/ 1dia
CETESB	0.34	0.54	0.70	0.81	0.91	0.74	0.42	0.72	0.78	0.82	0.85	1.14
GRIDF	0.28	0.49	0.73	0.86	0.93	0.73	0.50	0.79	0.82	0.86	0.88	1.14
Bias	-21%	-10%	4%	6%	2%	-1%	16%	9%	5%	5%	3%	0%

Table 1Comparison of ratios between CETESB and GRIDF datasets. Values of GRIDF in this table represent country averages. Bias was computed as (GRIDF – CETESB)/CETESB.

hourly extremes typically account for a large fraction of daily maxima, particularly in convective regions, while more gradual accumulation dominates in subtropical zones.

Longer duration ratios (6–12 hours relative to 24 hours) display more spatial uniformity, with values clustering near unity across most of the country. This indicates that half-day accumulations are generally representative of daily totals, regardless of climate regime. However, localized differences persist, especially along the coastal mountains of the Southeast and in parts of the Amazon, where orographic enhancement and mesoscale convective systems can extend rainfall durations and lower sub-daily ratios.

Table 1 compares the nationally averaged disaggregation coefficients derived in this study (GRIDF) with the fixed values traditionally recommended by CETESB. The results highlight systematic differences across durations, with GRIDF ratios generally lower at very short intervals (5–15 minutes) but higher for hourly to multi-hour scales. For example, at 5 and 10 minutes the GRIDF coefficients are 0.28 and 0.49, respectively, compared to 0.34 and 0.54 from CETESB, corresponding to underestimations of 21% and 10%. In contrast, the 1-hour to daily ratio is 0.50 in GRIDF versus 0.42 in CETESB, a substantial 16% increase that underscores the greater contribution of hourly extremes to daily totals in the observed records. It is important to note that durations of 5 and 10 minutes are primarily made from the fittings to the data and spatial interpolation results.

At intermediate durations such as 6–12 hours, GRIDF coefficients remain consistently higher than CETESB by 3–9%, reflecting the role of prolonged convective or mesoscale events that CETESB's constants fail to capture. By construction, both approaches converge at the daily scale (1.14), but the progression across shorter durations reveals the limitations of assuming uniform ratios nationwide. The GRIDF-derived coefficients suggest that short bursts are somewhat less dominant than implied by CETESB, whereas longer accumulations contribute more strongly, especially at the 1-hour and 6-hour scales. These differences are hydrologically significant, as they directly affect design storm estimates for urban drainage and flood modeling, potentially leading to overdesign at sub-hourly durations and underdesign at hourly scales if CETESB constants are applied indiscriminately.

3.2. Bias Correction

As shown in Figure 4, all four products reproduce the large-scale rainfall gradients across Brazil, with higher annual totals along the northern and northwestern Amazon Basin and lower values in the semi-arid Northeast and southern interior. Relative to the BR-DWGD benchmark, IMERG slightly overestimates rainfall in the southern Amazon and central Brazil, while CHIRPS

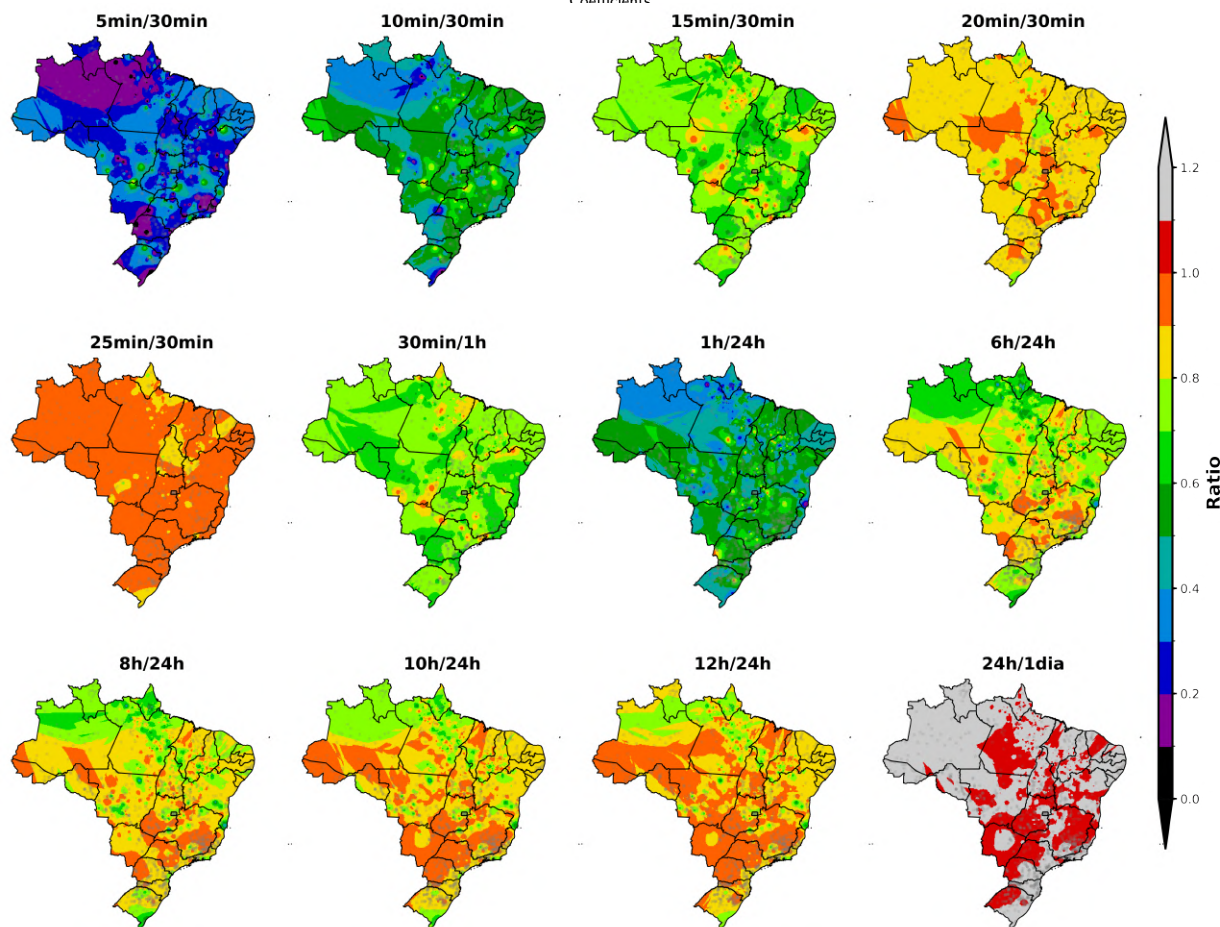


Figure 3: Spatial distribution of *sub-daily rainfall ratios* over Brazil. Panels (left→right, top→bottom) $P(5 \min)/P(30 \min)$. $P(10 \, \text{min})/P(30 \, \text{min}),$ $P(15 \min)/P(30 \min)$ $P(20 \min)/P(30 \min)$, P(25 min)/P(30 min), $P(30 \, \text{min})/P(1 \, \text{h})$ P(1 h)/P(24 h) $P(6 \, h)/P(24 \, h)$ P(8 h)/P(24 h), $P(10\,\mathrm{h})/P(24\,\mathrm{h}),\ P(12\,\mathrm{h})/P(24\,\mathrm{h}),\ \mathrm{and}\ P(24\,\mathrm{h})/P_{\mathrm{day}}.$ Gray dots indicate the gauges used in each panel (after resolution/quality screening); for the 5- and 10-min panels the short-duration values come from a polynomial model and are not constrained by native gauge resolution. Values are interpolated to a 0.1° grid using inverse-distance weighting (p = 2, k = 10 neighbors) and masked to Brazil; state boundaries are overlaid. The shared vertical color bar (right, 20 discrete bins, range 0.30-1.20) shows the dimensionless ratio $P(d_1)/P(d_2)$, where larger values indicate a greater fraction of the reference duration in the numerator relative to the denominator.

and PERSIANN-CDR display totals closer to the reference in these regions. In contrast, the semiarid Northeast and the coastal zones of the Southeast reveal stronger divergence: IMERG tends to produce wetter estimates, whereas PERSIANN-CDR shows drier conditions compared to BR-DWGD. Despite these regional differences, all datasets converge in capturing the spatial structure of rainfall maxima over the Amazon and the overall gradient toward drier conditions in the Northeast, with mean national averages differing by less than 5% relative to BR-DWGD.

Figure 5 illustrates the impact of multiplicative bias correction on the agreement between gridded rainfall products and station observations at the 98th percentile threshold, which targets the

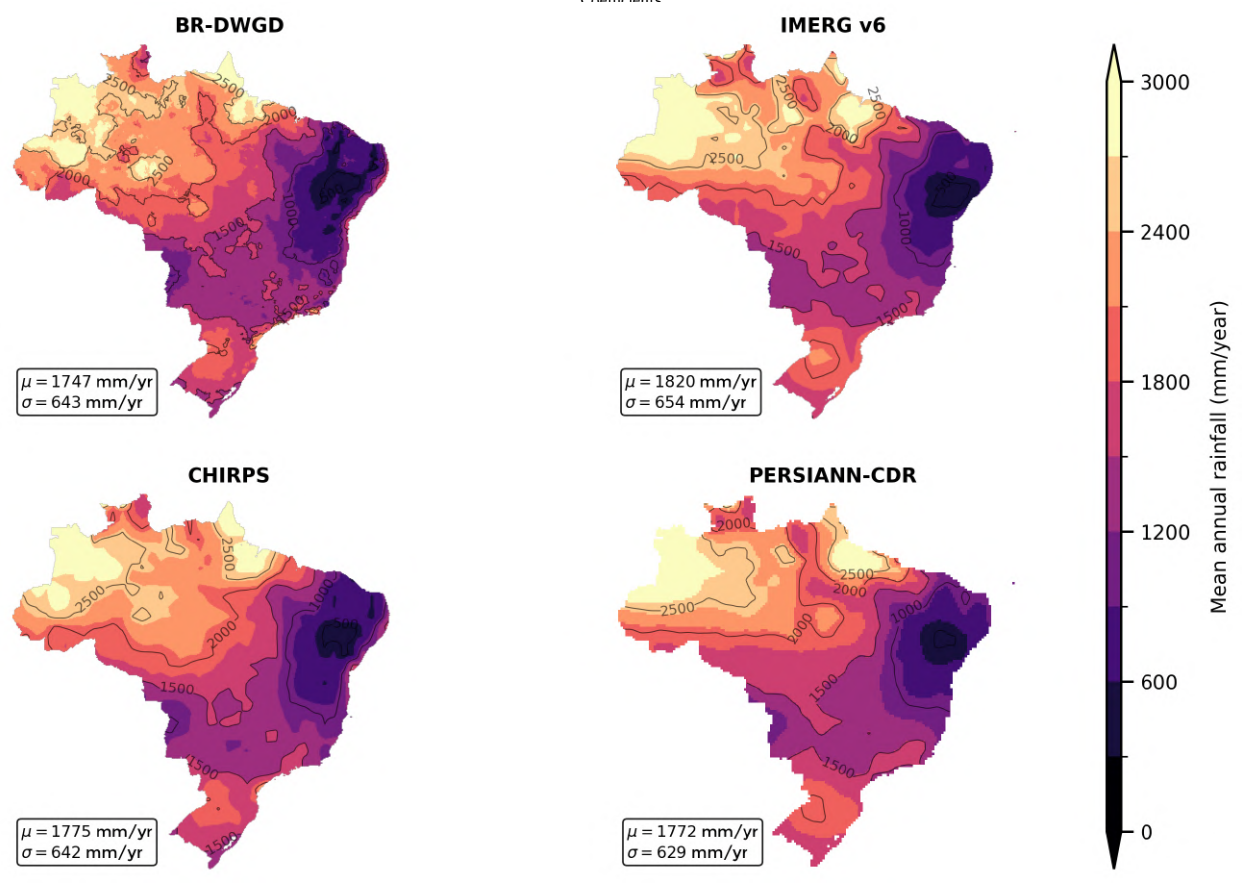


Figure 4: Annual average rainfall from 2000 to 2023 for different products.

upper tail of the rainfall distribution. The scatterplots in the left column show that all raw products systematically underestimate extremes, with regression slopes well below unity and substantial spread around the 1:1 line. For example, BR-DWGD raw values yielded a slope of 0.61 ($R^2 = 0.89$), which improved to 1.07 ($R^2 = 0.90$) after correction, while PERSIANN improved from a slope of 0.38 ($R^2 = 0.68$) to 0.94 ($R^2 = 0.72$). IMERG, although improved from 0.55 ($R^2 = 0.63$) to 1.13 ($R^2 = 0.64$), still exhibits larger scatter, and CHIRPS shows a similar trend, with slope increasing from 0.44 ($R^2 = 0.68$) to 1.02 ($R^2 = 0.72$). These results indicate that the bias correction effectively rescales magnitudes and reduces systematic underestimation, while also improving variance explained in most cases.

The maps of bias factors reveal coherent spatial patterns in the required corrections. BR-DWGD shows relatively minor adjustments, consistent with its dense gauge foundation, while IMERG and CHIRPS require stronger upscaling in northern Brazil and the semi-arid Northeast, where convective systems dominate. PERSIANN exhibits the largest corrections, with bias factors exceeding 2.5 in central and southern Brazil.

3.3. Comparison with existing IDFs

Figure 6 compares the bias between observed station-fitted and raster-derived IDF curves for selected durations (15, 60, 1440, and 7200 minutes) and return periods (10 and 25 years). The

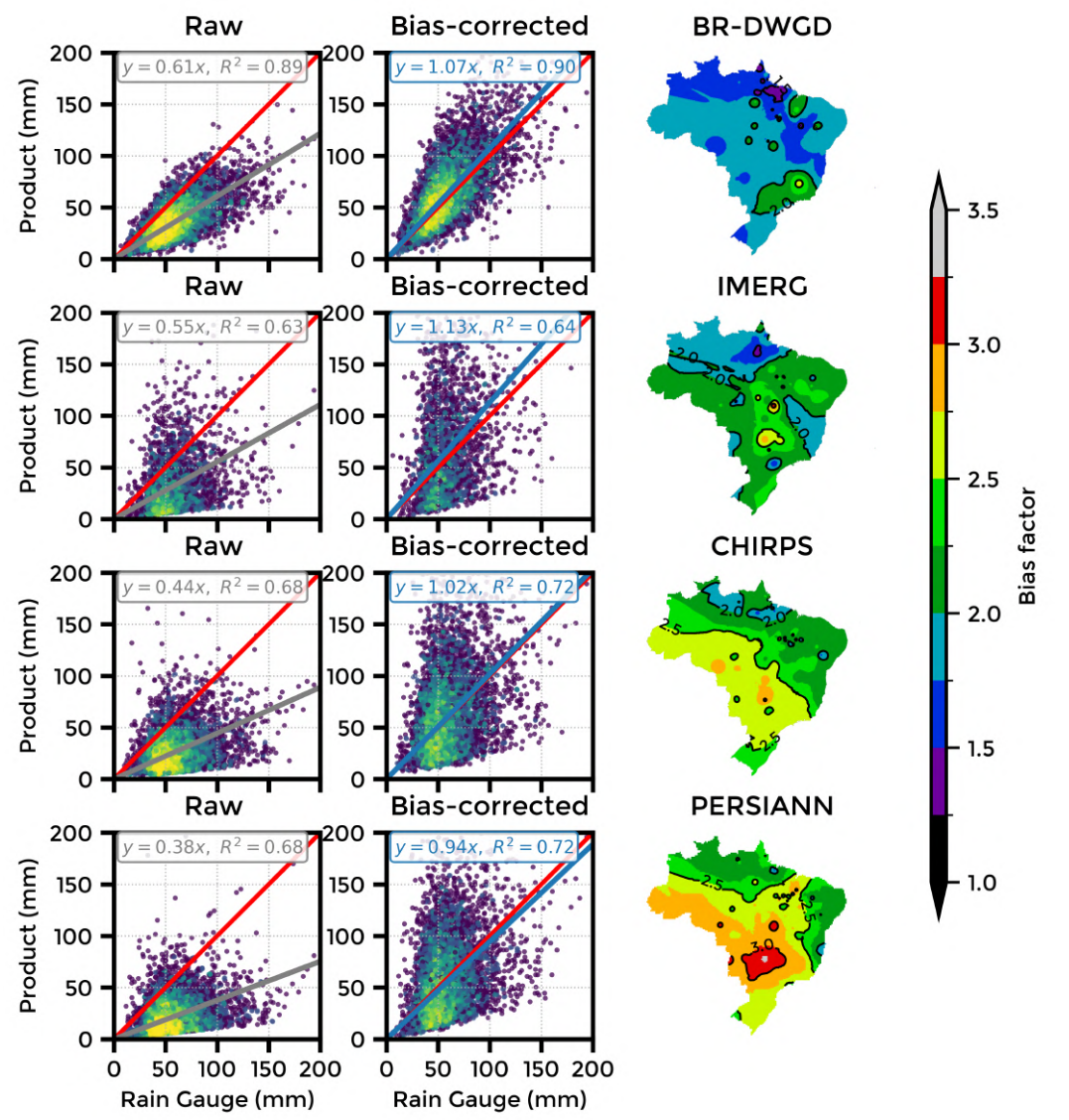


Figure 5: Bias correction for 98th percentile above rainfall using daily-resolution ANA rainfall stations. Rows correspond to BR-DWGD, IMERG, CHIRPS, and PERSIANN. Left column: raw product values (y) plotted against rain-gauge values (x). Middle column: bias-corrected values (ζP). All scatter panels share the same axis limits (0–200 mm). The red line is the 1:1 reference; the colored line is an origin-forced fit with slope a and R^2 . Point colors indicate sample density. Right column: spatial field of the multiplicative bias factor ζ over Brazil with state boundaries and contours at 0.5 resolution. A single vertical colorbar shows ζ (range 1–3.5). Values ζ < 1 indicate product overestimation; values ζ > 1 indicate underestimation requiring upscaling.

largest biases are observed at shorter durations (15 and 60 minutes), where IDFs estimated in this paper tend to overestimate rainfall intensities by more than 50% at several stations, for both disaggregation methods. For daily and multi-day durations (1440 and 7200 minutes), biases are generally lower in magnitude. Because positive but relatively lower biases are observed in the 1440 min duration (24h), and sub-daily rainfall is estimated with disaggregation coefficients,

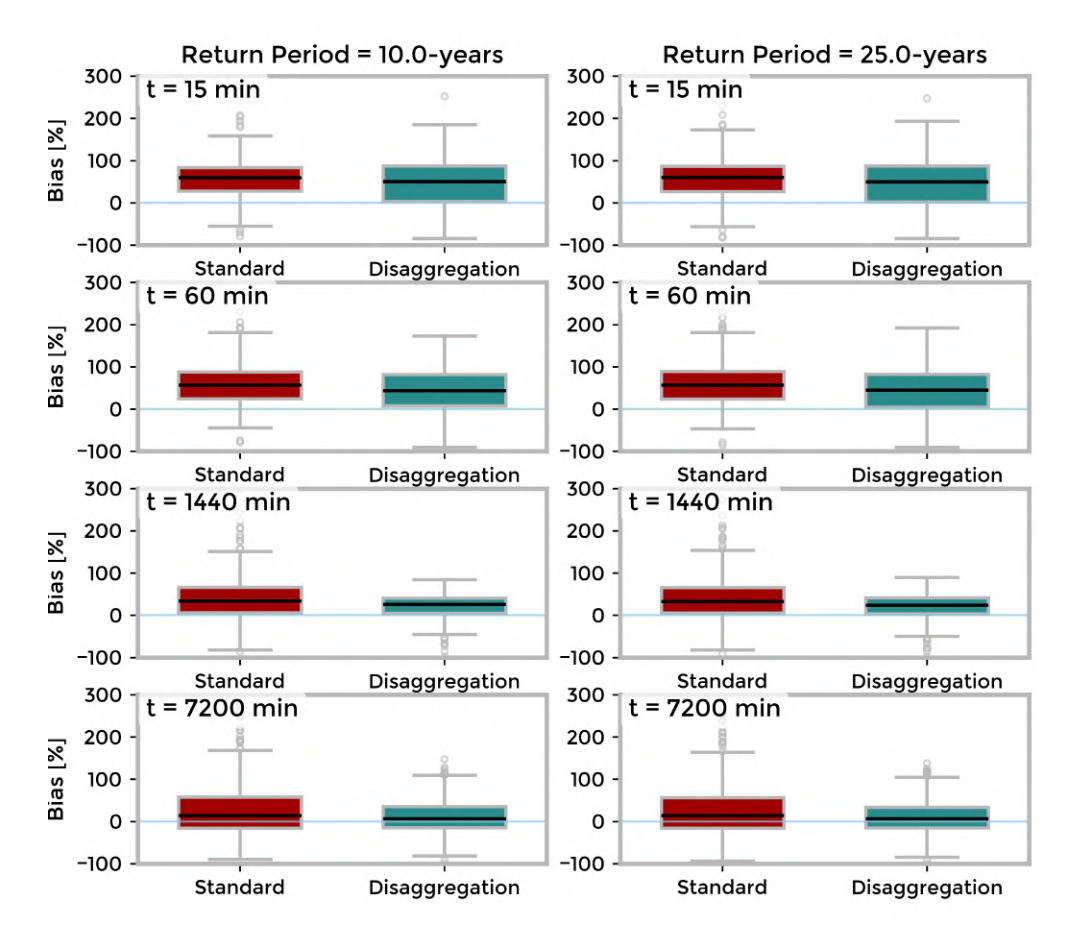


Figure 6: Boxplots of bias (%) between observed IDFs from daily rainfall (disaggregation) and with sub-daily rainfall (standard) from (Torres et al., 2025) to locally-derived IDF curves using BR-DWGD for selected durations (15, 60, 1440, and 7200 minutes) and return periods (10 and 25 years). The shaded zero line highlights unbiased agreement, while positive values indicate overestimation of intensities by the raster product relative to stations.

the differences in the median biases for sub-daily durations might be highly influenced by the disaggregation coefficients used. These results highlight the importance of incorporating locally derived disaggregation when estimating short-duration extremes, as it leads to more reliable and spatially consistent IDF curves across Brazil (Figure 6).

3.4. GRIDF - BR Toolbox

The GRIDF-BR Google Earth Engine interface was developed to provide an interactive platform for visualizing and comparing rainfall Intensity–Duration–Frequency (IDF) curves across Brazil. The tool allows users to select among multiple rainfall products (BR-DWGD, IMERG, CHIRPS, and PERSIANN), apply either raw or bias-corrected data, and choose the disaggregation method (locally derived, CETESB, or station-based). Users can then display spatial maps of IDF parameters or performance metrics (e.g., K, a, b, c, MSE, RMSE, R^2) and query individual grid

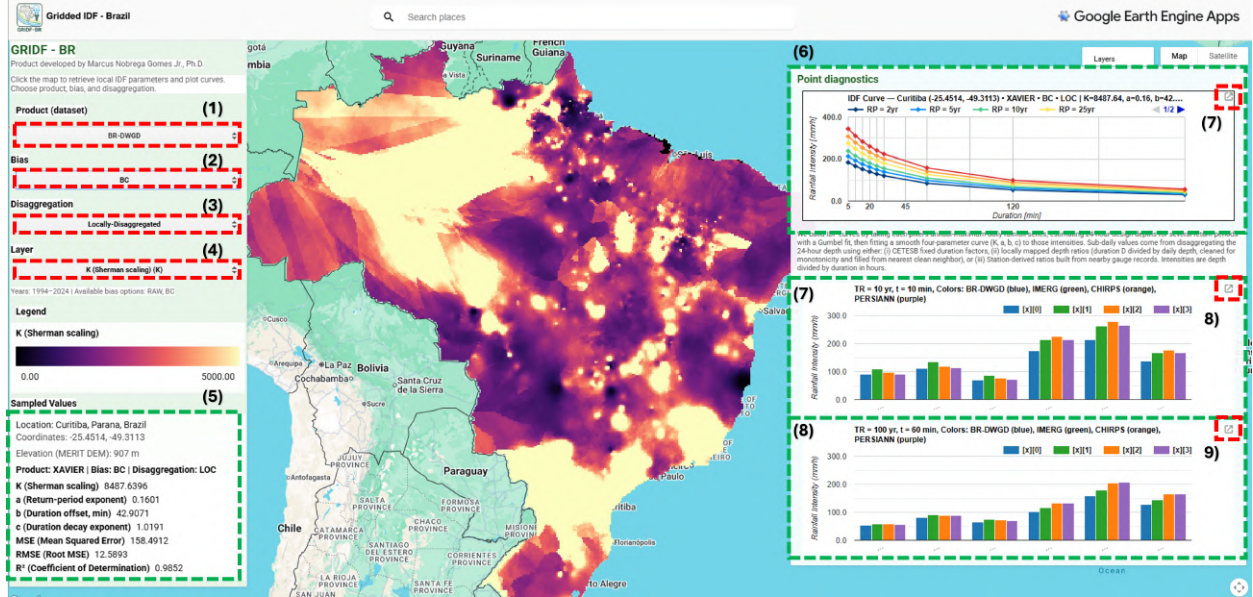


Figure 7: Overview of the GRIDF-BR Google Earth Engine interface. Panel (1) selects the rainfall product (BR-DWGD, IMERG, CHIRPS, or PERSIANN), followed by panel (2) for bias option (RAW or BC), and panel (3) for the disaggregation method (Locally-Disaggregated, CETESB, or Station-derived). Panel (4) chooses the IDF parameter or metric to visualize (K, a, b, c, MSE, RMSE, or R^2), while panel (5) reports sampled values at the clicked location, including coordinates, elevation, parameters, and model diagnostics. On the right side, panel (6) shows the IDF curve for the selected point, and panels (7)–(8) present grouped bar plots where each group corresponds to a bias-disaggregation combination and colors indicate datasets (blue: BR-DWGD, green: IMERG, orange: CHIRPS, purple: PERSIANN). All charts can be downloaded in SVG or PNG formats, or exported as CSV tables. The tool can be accessed in https://gridf-470516.projects.earthengine.app/view/gridf-br.

cells to obtain detailed diagnostics including coordinates, elevation through MERIT DEM (Yamazaki et al., 2019), fitted parameters, and quality statistics. The interface also generates IDF curves for user-defined points and grouped bar plots to compare products across bias—disaggregation combinations. All outputs can be exported in graphical (SVG or PNG) or tabular (CSV) formats, enabling flexible integration with external analyses (Figure 7).

4. Discussion

Reliable Intensity—Duration—Frequency (IDF) curves are essential for urban planning, stormwater design, and flood risk management, yet the absence of updated, nationally consistent tools in Brazil has left many designs vulnerable to underestimation or overestimation of extremes. Recent unprecedented catastrophic floods in Rio Grande do Sul highlight how inadequate design standards can amplify human and economic losses (Marengo et al., 2024; Collischonn et al., 2025). Unlike countries such as the United States, which benefits from NOAA's Atlas 14 and long-term sub-daily networks (Atlas, 14), Brazil lacks a unified national framework and high-resolution datasets to fully characterize and spatially resolve the role of short-duration rainfall. Despite these constraints, advances in rain gauge networks and satellite-based products now allow us to construct

high-resolution, bias-corrected gridded IDF curves for the entire country, even in the face of these limitations. While certainly not free of uncertainties, these datasets provide an operational platform for evaluating storm intensity, comparing methods, and quantifying uncertainty. This step forward can improve the reliability of design decisions and enhance resilience in Brazilian cities increasingly exposed to short, intense convective storms.

The results of our analysis show that short-duration rainfall events contribute a large part of the daily maximum. On average, 1-hour accumulations represent about 56% of the daily total, while sub-hourly bursts contribute 30–40%. This confirms the importance of convective storms in shaping extremes and indicates that using constant national disaggregation coefficients, such as those from CETESB, can lead to systematic underestimation for several sub-daily durations. Locally derived values are therefore needed to represent the contribution of short durations and to produce more reliable IDF curves for design.

The spatial analysis of disaggregation ratios indicates variability across regions, but clear climatic patterns are difficult to isolate with the current quality controlled gauge network. The uneven distribution of stations, combined with differences in record quality and length, limits the ability to fully characterize regional controls on short-duration rainfall or to define smooth regions to apply regionalized disaggregation coefficients. For this reason, we present not only results using rasterized disaggregation coefficients, but also constraining the grid cells to use the coefficients of the closest quality-controlled station. It is likely that with a denser and more quality-controlled rain gauge network, more consistent spatial patterns would emerge without the influence of spatial interpolation artifacts. Despite these limitations, the results confirm that disaggregation is not uniform nationwide, and that applying fixed coefficients introduces bias. Nonetheless, even with the interpolated fields of disaggregation coefficients developed in this paper, national averages of these coefficients remained virtually larger than CETESB for all durations larger than 15-min - the higher rain gauge resolution used in this analysis. This clearly suggests evidence that short extreme rainfall extremes might be higher than those proposed by CETESB in 1986 for the recent climate.

Satellite products show good convergence when estimating annual mean rainfall, with averages generally consistent across datasets and with BR-DWGD. However, agreement at the long-term annual mean does not extend to the tails of the distribution. The analysis of extremes reveals substantial differences between products, particularly for short durations and high return periods. This highlights that while satellite data are useful for capturing broad spatial and temporal patterns of precipitation, careful bias correction and validation against gauges are required before they can be reliably used for IDF estimation.

The comparison between stations and gridded products shows that raw datasets, including BR-DWGD, IMERG, CHIRPS, and PERSIANN, consistently underestimate rainfall extremes. Applying multiplicative bias correction improves the agreement with observations, reducing systematic errors and narrowing the spread between products. These results confirm that bias correction is necessary for both satellite-based and gauge-interpolated datasets before they are used in IDF estimation.

Most of the IDF equations historically available for Brazil were developed using past climate records, with only a limited number extending beyond the year 2000. The compilation by Torres et al. (2025) shows that more than 6500 IDF equations exist nationwide, but the majority were derived either from short pluviographic series or through the disaggregation of daily rainfall using diverse empirical methods for disaggregation from national, regional, to local disaggregation

methods. Consequently, differences among published IDF curves may reflect methodological inconsistencies and data limitations as much as real hydroclimatic variability. This limitation underscores the need for updated IDFs based on quality-controlled, long-term records and standardized methods, ensuring comparability and reliability across regions.

The GRIDF-BR toolbox developed in Google Earth Engine provides a practical means of applying the methods presented in this study. Through an interactive interface (Figure 7), users can explore IDF parameters across multiple rainfall products, compare raw and bias-corrected datasets, and select different disaggregation approaches. The tool generates maps, station-level diagnostics, and IDF curves that can be exported for further analysis, making the results directly accessible to practitioners. The toolbox has several practical applications beyond IDF curve generation. At the engineering level, it can be used to design and test urban drainage systems by providing updated rainfall intensities for multiple durations and return periods. Because the spatial resolution of the datasets allows for several grid cells to cover a single metropolitan area, the tool also enables the assessment of subgrid climate variability within cities, an important factor in local-scale planning. By allowing users to compare different rainfall products, bias-correction options, and disaggregation methods, the toolbox supports a more explicit evaluation of uncertainty in rainfall extremes, which is critical for risk-informed design. In addition, its accessible interface and direct visualization capabilities make it a valuable educational platform for teaching hydrology, climate adaptation, and water resources planning.

5. Conclusions

This study addressed the urgent need for updated and spatially consistent IDF curves in Brazil, where most existing equations are based on outdated climate records and heterogeneous disaggregation methods. We combined BR-DWGD daily maxima (1994–2024) with locally derived disaggregation coefficients and applied multiplicative bias correction to satellite products (IMERG, CHIRPS, and PERSIANN) in order to produce a consistent framework for IDF estimation. The approach was implemented in the GRIDF-BR toolbox, an open platform developed in Google Earth Engine to support practitioners and researchers.

The results demonstrate that short-duration rainfall contributes substantially to daily totals, with 1-hour extremes accounting on average for 56% of the daily maximum (16% larger than the national standard) and sub-hourly bursts contributing 30–40%. Uniform coefficients, such as those from CETESB, fail to capture this contribution and systematically underestimate or overestimate intensities. Bias correction using the 98th percentile as a threshold to define extreme events improved agreement between gridded products and rain gauges. All uncorrected gridded products systematically underestimated daily extremes. Applying a multiplicative bias adjustment improved agreement with gauges, yielding parity slopes close to unity: *BR-DWGD* improved from 0.61 to 1.07, *IMERG* from 0.55 to 1.13, *CHIRPS* from 0.44 to 1.02, and *PERSIANN* from 0.38 to 0.94.

The findings of this study have relevant implications for hydraulic design and urban planning. The proposed framework provides a consistent basis for estimating IDF relationships at the national scale, which may help reduce the risk of underestimating design storms and improve infrastructure planning in flood-prone areas. The GRIDF-BR toolbox operationalizes these results by enabling IDF extraction, product inter-comparison, and visualization at municipal and basin scales. Nevertheless, some limitations should be noted: the availability and quality of sub-daily

rainfall records remain uneven across Brazil, and in many regions long-term, high-resolution data are still lacking to fully characterize storm dynamics. Future research could focus on testing more advanced bias-correction approaches and incorporating climate change scenarios so that IDF curves reflect both present and projected conditions. Expanding and improving the network of high-quality sub-daily rainfall measurements will also be essential for better representing the short, intense events that drive urban flood risk and constitute critical inputs for design and adaptation.

Data and Tool Availability

All datasets and tools used in this study are openly accessible and can be found in an open repository https://github.com/marcusnobrega-eng/GRIDF. Daily rainfall fields were obtained from BR-DWGD (Xavier et al., 2022), CHIRPS (https://www.chc.ucsb.edu/data/chirps, GEE: UCSB-CHG/CHIRPS/DAILY), IMERG V07 (NASA GES DISC/PPS, GEE: NASA/GPM_L3/IMERG_V07 and PERSIANN-CDR (NOAA NCEI, CHRS: https://chrsdata.eng.uci.edu). Sub-daily records for disaggregation were retrieved from the ANA telemetric network (Hidroweb/Telemetria). The GRIDF-BR toolbox for interactive IDF retrieval is available on Google Earth Engine at https://gridf-470516.projects.earthengine.app/view/gridf-br . Processing scripts for data handling, bias correction, and IDF fitting will be released on GitHub under an MIT license.

Acknowledgment

The authors gratefully acknowledge the Brazilian National Water Agency (ANA) for granting permission to access and use the telemetric rainfall database through its API. We also thank NASA GES DISC/PPS for providing IMERG data, the Climate Hazards Center (University of California, Santa Barbara) for CHIRPS, NOAA's National Centers for Environmental Information (NCEI) and the Center for Hydrometeorology and Remote Sensing (CHRS, University of California, Irvine) for PERSIANN-CDR, and the developers of the BR-DWGD dataset for making daily gridded rainfall fields available.

CRediT authorship contribution statement

Marcus Nóbrega Gomes Jr.: Conceptualization, Methodology, Software, Validation, Formal analysis, Investigation, Data Curation, Writing - Original Draft, Writing - Review & Editing, Visualization.

References

- Almeida, W.S.d., Corrêa, F.V., Caminha, A.R., Oliveira, M.C.F.d., Carvalho, D.F.d., Oliveira, L.F.C.d., 2025. The use of rainfall disaggregation coefficients to obtain intensity-duration-frequency curves: estimation using pluviographic data versus national mean values. Revista Ambiente & Água 20, e3061.
- Alsumaiti, T.S., Hussein, K.A., Ghebreyesus, D.T., Petchprayoon, P., Sharif, H.O., Abdalati, W., 2023. Development of intensity–duration–frequency (idf) curves over the united arab emirates (uae) using chirps satellite-based precipitation products. Remote Sensing 16, 27.
- Aragão, R.d., Costa, F.F.d., Rufino, I.A., Ramos Filho, R.d.S., Srinivasan, V.S., Truta, J.d.B., 2024. Intensity-duration-frequency equations (idf) for the state of paraíba, brazil, and regionalization of its parameters. Revista Brasileira de Engenharia Agrícola e Ambiental 28, e283679.
- Arnbjerg-Nielsen, K., Willems, P., Olsson, J., Beecham, S., Pathirana, A., Bülow Gregersen, I., Madsen, H., Nguyen, V.T.V., 2013. Impacts of climate change on rainfall extremes and urban drainage systems: a review. Water science and technology 68, 16–28.
- Ashouri, H., Hsu, K.L., Sorooshian, S., Braithwaite, D.K., Knapp, K.R., Cecil, L.D., Nelson, B.R., Prat, O.P., 2015. Persiann-cdr: Daily precipitation climate data record from multisatellite observations for hydrological and climate studies. Bulletin of the American Meteorological Society 96, 69–83.
- Atlas, N., 14. Precipitation-frequency atlas of the united states. Multiple Volumes, National Weather Service, Silver Spring Maryland. Back, Á.J., Cadorin, S.B., Galatto, S.L., 2020. Extreme rainfall and idf equations for alagoas state, brazil. Revista Ambiente & Água 15, e2544.

- Ballarin, A.S., Anache, J.A., Wendland, E., 2022a. Trends and abrupt changes in extreme rainfall events and their influence on design quantiles: a case study in são paulo, brazil. Theoretical and Applied Climatology 149, 1753–1767.
- Ballarin, A.S., Calixto, K.G., Anache, J.A., Wendland, E., 2022b. Combined predictive and descriptive tests for extreme rainfall probability distribution selection. Hydrological Sciences Journal 67, 1130–1140.
- Ballarin, A.S., Wendland, E., Zaerpour, M., Hatami, S., Meira Neto, A.A., Papalexiou, S.M., 2024. Frequency rather than intensity drives projected changes of rainfall events in brazil. Earth's Future 12, e2023EF004053.
- Berger, V.W., Zhou, Y., 2014. Kolmogorov-smirnov test: Overview. Wiley statsref: Statistics reference online .
- Bibi, T.S., Tekesa, N.W., 2023. Impacts of climate change on idf curves for urban stormwater management systems design: The case of dodola town, ethiopia. Environmental Monitoring and Assessment 195, 170.
- de Bodas Terassi, P.M., Pontes, P.R.M., Xavier, A.C.F., Cavalcante, R.B.L., de Oliveira Serrão, E.A., Sobral, B.S., de Oliveira-Júnior, J.F., de Melo, A.M.Q., Baratto, J., 2023. A comprehensive analysis of regional disaggregation coefficients and intensity-duration-frequency curves for the itacaiúnas watershed in the eastern brazilian amazon. Theoretical and Applied Climatology 154, 863–880.
- Boulomytis, V.T.G., Zuffo, A.C., Imteaz, M.A., 2018. Derivation of design rainfall and disaggregation process of areas with limited data and extreme climatic variability. International Journal of Environmental Research 12, 147–166.
- Butcher, J.B., Zi, T., Pickard, B.R., Job, S.C., Johnson, T.E., Groza, B.A., 2021. Efficient statistical approach to develop intensity-duration-frequency curves for precipitation and runoff under future climate. Climatic change 164, 3.
- Caldeira, T.L., Beskow, S., de Mello, C.R., Vargas, M.M., Guedes, H.A.S., Faria, L.C., 2015. Daily rainfall disaggregation:: An analysis for the rio grande do sul state. Scientia agraria 16, 1–21.
- Campos, A.R., Silva, J.B.L.d., Santos, G.G., Ratke, R.F., Aquino, I.O.d., 2017. Estimate of intense rainfall equation parameters for rainfall stations of the paraíba state, brazil. Pesquisa Agropecuária Tropical 47, 15–21.
- Carvalho, W., 2020. Hydrobr: A python package to work with brazilian hydrometeorological time series. Disponível: https://doi. org/10.5281/zenodo 3931027.
- Carvalho Abreu, M., Thebit de Almeida, L., Bernardes Silva, F., de Souza Fraga, M., Bastos Lyra, G., Souza, A., da Silva, D.D., Avelino Cecílio, R., 2023. Disaggregation coefficients for obtaining rainfall intensity-duration-frequency curves: concepts, models, errors and trends in minas gerais, brazil. Urban Water Journal 20, 1647–1660.
- Coelho, M.M., de Figueiredo, N.M., de Medeiros Coelho, M.T., Campos Filho, L.C.P., 2023. Rainfall intensity model with spatialization of intensity-duration-frequency curve parameters-a case study for the state of maranhão, brazil. Acta Scientiarum. Technology 45, e63369.
- Collischonn, W., Fan, F.M., Possantti, I., Dornelles, F., Paiva, R., Medeiros, M.S., Michel, G.P., Magalhães Filho, F.J.C., Moraes, S.R., Marcuzzo, F.F.N., et al., 2025. O desastre hidrológico excepcional de abril-maio de 2024 no sul do brasil. RBRH 30, e1.
- Cook, L.M., McGinnis, S., Samaras, C., 2020. The effect of modeling choices on updating intensity-duration-frequency curves and stormwater infrastructure designs for climate change. Climatic change 159, 289–308.
- Cooray, K., 2010. Generalized gumbel distribution. Journal of Applied Statistics 37, 171-179.
- Dodman, D., Hayward, B., Pelling, M., Castán Broto, V., Chow, W., Chu, E., Dawson, R., Khirfan, L., McPhearson, T., Prakash, A., et al., 2023. Cities, settlements and key infrastructure.
- Funk, C., Peterson, P., Landsfeld, M., Pedreros, D., Verdin, J., Shukla, S., Husak, G., Rowland, J., Harrison, L., Hoell, A., et al., 2015. The climate hazards infrared precipitation with stations—a new environmental record for monitoring extremes. Scientific data 2, 1–21.
- Ghebreyesus, D.T., Sharif, H.O., 2021. Development and assessment of high-resolution radar-based precipitation intensity-duration-curve (idf) curves for the state of texas. Remote Sensing 13, 2890.
- Handmer, J., Honda, Y., Kundzewicz, Z.W., Arnell, N., Benito, G., Hatfield, J., Mohamed, I.F., Peduzzi, P., Wu, S., Sherstyukov, B., et al., 2012. Changes in impacts of climate extremes: human systems and ecosystems. Managing the risks of extreme events and disasters to advance climate change adaptation special report of the intergovernmental panel on climate change, 231–290.
- Huffman, G.J., Bolvin, D.T., Braithwaite, D., Hsu, K., Joyce, R., Kidd, C., Nelkin, E., Sorooshian, S., Tan, J., Xie, P., 2023. Nasa global precipitation measurement (gpm) integrated multi-satellite retrievals for gpm (imerg) version 07. Algorithm Theoretical Basis Document (ATBD) Version 47.
- Kandalai, S., John, N.J., Patel, A., 2023. Effects of climate change on geotechnical infrastructures—state of the art. Environmental Science and Pollution Research 30, 16878–16904.
- Lau, A., Behrangi, A., 2022. Understanding intensity-duration-frequency (idf) curves using imerg sub-hourly precipitation against dense gauge networks. Remote Sensing 14, 5032.
- Lima, V.d.S., Tavares, P.R.L., Batista, T.L., 2021. Ajuste e validação de equações idf a partir de dados pluviométricos para cidades do estado de pernambuco, brasil. Revista Brasileira de Meteorologia 36, 713–721.
- Marengo, J.A., Dolif, G., Cuartas, A., Camarinha, P., Gonçcalves, D., Luiz, R., Silva, L., Alvala, R.C., Seluchil, M.E., Moraes, O.L., et al., 2024. O maior desastre climático do brasil: Chuvas e inundações no estado do rio grande do sul em abril-maio 2024. Estudos Avançados 38, 203–228.
- Mascaro, G., Farris, S., Deidda, R., 2025. Evidence of emerging increasing trends in observed subdaily heavy precipitation frequency in the united states. Geophysical Research Letters 52, e2024GL114292.
- Mianabadi, A., 2023. Evaluation of long-term satellite-based precipitation products for developing intensity-frequency (if) curves of daily precipitation. Atmospheric Research 286, 106667.
- das Neves Almeida, C., Francis Bertrand, G., Carvalho Lemos, F., da Silva Freitas, E., Lins Silva, A., Vidal Barbosa, J.L., Meira, M.A., Ramos Filho, G.M., Barbosa Athayde Junior, G., D'Castro Filho, F.J., et al., 2025. The design of the brazilian sub-daily rainfall dataset (br-sdr): two decades of high-time-resolution data in brazil. Hydrological Sciences Journal.
- Nunes, A.d.A., Pinto, E.J.d.A., Baptista, M.B., Paula, M.H.d., Xavier, M.O., 2021. Intensity-duration-frequency curves in the municipality of belo horizonte from the perspective of non-stationarity. RBRH 26, e29.
- Ombadi, M., Nguyen, P., Sorooshian, S., Hsu, K.I., 2018. Developing intensity-duration-frequency (idf) curves from satellite-based precipitation: Methodology and evaluation. Water Resources Research 54, 7752–7766.

- Pansera, W.A., Gomes, B.M., 2025. Performance of multiparameter distributions in estimating rainfall extremes and deriving idf equations in paraná.
- Penner, G.C., Wendland, E.C., Gonçalves, M.M., Adam, K.N., 2023. Methodology for idf equation based on reduced pluviograph records. Revista Brasileira de Ciências Ambientais, 365–374.
- Rodrigues, A.A., Siqueira, T.M., Beskow, T.L.C., Beskow, S., Mello, C.R.d., 2023. Intensity-duration-frequency equations for rio grande do sulbrazil, based on stationary rainfall series. Revista Ambiente & Água 18, e2878.
- Rodrigues, A.A., Siqueira, T.M., Beskow, T.L.C., Timm, L.C., 2024. Ordinary cokriging applied to generate intensity-duration-frequency equations for rio grande do sul state, brazil. Theoretical and Applied Climatology 155, 2365–2378.
- de Saneamento, C.C.d.T., et al., 1986. Drenagem urbana: Manual de projeto .
- Sherman, C.W., 1931. Frequency and intensity of excessive rainfalls at boston, massachusetts. Transactions of the American Society of Civil Engineers 95, 951–960.
- Silva, D.F., Goldenfum, J.A., Simonovic, S.P., Dornelles, F., 2023. Impacts of climate change on the intensity-duration-frequency curves of two urbanized areas in brazil using the high-resolution eta atmospheric model. Urban Water Journal 20, 123–139.
- Silveira, A.L.L.d., 2000. Equação para os coeficientes de desagregação de chuva. Rbrh: Revista Brasileira de Recursos Hídricos. Porto Alegre, RS. Vol. 5, n. 4 (out./dez. 2000), p. 143-147.
- Simoes-Sousa, I.T., Camargo, C.M., Tavora, J., Piffer-Braga, A., Farrar, J.T., Pavelsky, T.M., 2025. The may 2024 flood disaster in southern brazil: Causes, impacts, and swot-based volume estimation. Geophysical Research Letters 52, e2024GL112442.
- de Souza, V.A.S., Dias, R.H.S., da Silva Filho, E.P., Nunes, M.L.A., Andrade, C.D., da Rosa, A.L.D., 2016. Determining idf equations for the state of rondônia. Revista Brasileira de Climatologia 18.
- de Souza Costa, C.E.A., Blanco, C.J.C., de Oliveira-Júnior, J.F., 2020. Idf curves for future climate scenarios in a locality of the tapajós basin, amazon, brazil. Journal of Water and Climate Change 11, 760–770.
- Stein, L., Mukkavilli, S.K., Pfitzmann, B.M., Staar, P.W., Ozturk, U., Berrospi, C., Brunschwiler, T., Wagener, T., 2024. Wealth over woe: Global biases in hydro-hazard research. Earth's Future 12, e2024EF004590.
- Tamm, O., Saaremäe, E., Rahkema, K., Jaagus, J., Tamm, T., 2023. The intensification of short-duration rainfall extremes due to climate change–need for a frequent update of intensity–duration–frequency curves. Climate services 30, 100349.
- Torres, I.P., Cecílio, R.A., de Almeida, L.T., Abreu, M.C., da Silva, D.D., Zanetti, S.S., Xavier, A.C., 2025. Rainfall intensity–duration–frequency curves dataset for brazil. Data 10, 17.
- Venkatesh, K., Maheswaran, R., Devacharan, J., 2022. Framework for developing idf curves using satellite precipitation: a case study using gpmimerg v6 data. Earth Science Informatics 15, 671–687.
- Xavier, A.C., Scanlon, B.R., King, C.W., Alves, A.I., 2022. New improved brazilian daily weather gridded data (1961–2020). International Journal of Climatology 42, 8390–8404.
- Yamazaki, D., Ikeshima, D., Sosa, J., Bates, P.D., Allen, G.H., Pavelsky, T.M., 2019. Merit hydro: A high-resolution global hydrography map based on latest topography dataset. Water Resources Research 55, 5053–5073.
- Yan, L., Xiong, L., Jiang, C., Zhang, M., Wang, D., Xu, C.Y., 2021. Updating intensity–duration–frequency curves for urban infrastructure design under a changing environment. Wiley Interdisciplinary Reviews: Water 8, e1519.